Pergamon

Int. J. Heat Mass Transfer. Vol. 37, No. 13, pp. 1849–1855, 1994

0017-9310/94 $7.00+0.00

0017-9310(94)E0014-L

Effects of wall conduction and interface thermal resistance on the phase-change problem

CHI-CHUAN HWANG, SENPUU LIN and LI-FU SHEN

Department of Mechanical Engineering, Chung Yuan University, Chung Li, Taiwan 32023, Republic of China

(*Received for publication* 20 *January* 1994)

Abstract—Perturbation solutions for the phase-change problem during solidification involving the wall conduction and wall–material interfacial thermal contact resistance boundary condition are presented in a straightforward approximate analytical manner. Comparison is made between the present result and those in the case with neglecting the effects of wall–material interfacial thermal resistance and/or wall conduction. It is found that the solidification rate increases with decreasing wall–material interfacial thermal resistance, or increasing Stefan number, or decreasing the ratio of solidified-material thermal conductivity to wall thermal conductivity.

INTRODUCTION

THE HEAT-TRANSFER problems involving phase change with the wall conduction and wall–material interfacial thermal contact resistance boundary condition are of particular interest in applications such as ice formation, freezing food, solidification of castings and ingots, metallurgy, the crystal growth from melts, and various other solidification technologies. For example, during formation of ice, the heat extracted from the liquid and the latent heat of solidification liberated at the solid–liquid interface are transferred across the solid phase, the solid–mold interface, and the mold, encountering at each one of these steps a certain thermal resistance. As the water solidifies, an air gap may form due to the imperfect solid–mold contact and a lubricant may sometimes be used to facilitate removal of the solidified ice from the mold. The prediction of temperature distributions and solidification/melting rate is very important in some modern technologies in order to control the fundamental parameters such as the speed of fabrication, the incidence of defects, as well as the influence on final properties of products and on the possibility of damage to the wall–material interface contact surface. But many important physical heat-transfer processes that occur across interfaces during solidification/melting have not been adequately studied and are not well understood. An exact analysis [1, 2] has been presented to treat the generalized unidirectional solidification problem subject only to the constraint that the metal–mold interfacial thermal contact resistance (heat transfer coefficient) be invariant. The technique involves the mathematical expedient of representing components of the interfacial thermal resistance by virtual layers of solid metal and/or mold. It is demonstrated [3] that the kinetic and thermal description of the model reduces to the expected one in three simple limiting cases. Viskanta reviewed the heat transfer problems of phase change with/without the mold–metal interface during melting and solidification of metals [4].

However, mathematical modeling is a powerful tool to aid in the task of understanding and control of complex processes during solidification and melting. Due to the non-linear boundary condition at the solid–liquid interface and the superimposition of wall–material interfacial thermal resistance, exact analytical solutions are limited to a few simple cases. Therefore, approximate, semi-analytical and numerical methods must be used to solved the phase-change problems [5, 6]. Application of perturbation methods in transient heat-transfer problems needs special attention. Pedroso and Domoto [7, 8] successfully adopted the perturbation method in solving the solidification problem of saturated liquid with planar and spherical geometries. Huang and Shih [9] obtained the perturbation solutions during the freezing on a flat plate with constant wall temperature in a straightforward manner. Yan and Huang [10] applied the perturbation method to phase change problem subject to convection and radiation. Aziz and Na [11] provided a heat transfer oriented approach to perturbation techniques. Aziz and Lunardini [12] reviewed the importance and usefulness of the perturbation method in phase-change heat-transfer problems.

In the present investigation, the perturbation technique is extended to the phase-change problem involving the wall conduction and constant wall–material interfacial thermal contact resistance boundary condition during solidification of material. The temperature distributions of wall and solidified-material, as well as the speed, of the solid–liquid interface are to be determined and expressed in analytical forms. Comparison is made between the present result and

NOMENCLATURE

C_p	specific heat at constant pressure
erf	error function
g	dimensionless solidification rate, $dH/d\tau$
h	position of solid–liquid interface
H	dimensionless position of solid–liquid interface, h/l
k	thermal conductivity
l	thickness of the wall
L	latent heat of solidification
r	thermal contact resistance at the wall–material interface
R	dimensionless thermal contact resistance, $k_s r/l$
t	time
T	absolute temperature in solidified-material or wall
T_f	solidification temperature of material
T_0	left-hand side wall surface temperature
x	space coordinate
X	dimensionless space coordinate, x/l.

Greek symbols

α	thermal diffusivity, $k/\rho C_p$
β	the ratio of thermal diffusivity of solidified-material to wall, α_s/α_w
ε	Stefan number, $C_{ps}(T_f - T_0)/L$
ζ	the ratio of thermal conductivity of solidified-material to wall, k_s/k_w
θ	dimensionless temperature, $(T-T_0)/(T_f-T_0)$
λ	root of equation (63)
ρ	density
τ	dimensionless time, $\varepsilon\alpha_s t/l^2$
τ^*	$\tau/\varepsilon = \beta_s t/l^2$.

Subscripts

s	solidified-material
w	wall.

those in the case with neglecting the effects of wall–material interfacial thermal resistance and/or wall conduction. Furthermore, we also discuss the effects of varying the thermal resistance, the Stefan number and the ratio of thermal conductivity of materials on the process.

ANALYSIS

The geometric configuration and the coordinate system for a solidification process, with a homogeneous wall of thickness l, with which we are concerned is schematically shown in Fig. 1. To simplify the analysis, the following fundamental assumptions are introduced [1, 2, 12]:

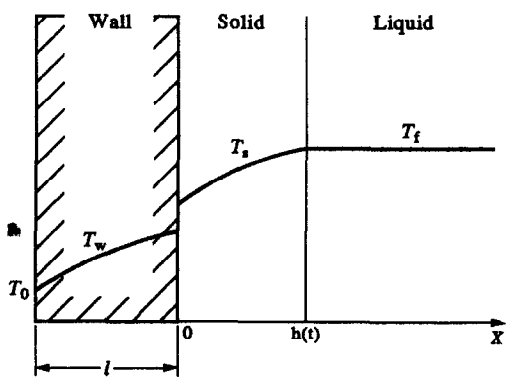

FIG. 1. Schematic model for the solidification process with wall conduction.

(1) conduction is the only heat-transfer mode and unidirectional;
(2) a thermal contact resistance, r, exists at the wall–material interface and remains constant throughout the process;
(3) both solid and liquid phases are homogeneous and isotropic;
(4) the material solidifies with a macroscopically planar solid–liquid interface and at the solidification temperature, T_f;
(5) superheat is assumed negligible and spurious heat losses from the liquid, by convection and radiation, are small and assumed negligible; and
(6) the thermal properties of material and wall are independent of both position and time.

In a plane coordinate system with the origin at the stationary wall–solid interface, the one-dimensional heat conduction describing the solidification process can be written in the following form:

$$\frac{\partial^2 T_s}{\partial x^2}(x,t) = \frac{1}{\alpha_s}\frac{\partial T_s}{\partial t}(x,t) \quad 0 \leqslant x \leqslant h(t), \tag{1}$$

$$T_s(x,t) = T_f \quad \text{at } x = h(t), \tag{2}$$

$$k_s \frac{\partial T_s}{\partial x}(x,t) = \rho_s L \frac{dh}{dt} \quad \text{at } x = h(t), \tag{3}$$

$$\frac{\partial^2 T_w}{\partial x^2}(x,t) = \frac{1}{\alpha_w}\frac{\partial T_w}{\partial t}(x,t) \quad -l \leqslant x \leqslant 0, \tag{4}$$

$$T_w(x,t) = T_0 \quad \text{at } x = -l, \tag{5}$$

$$k_s \frac{\partial T_s}{\partial x}(x,t) = \frac{T_s(x,t) - T_w(x,t)}{r} \quad \text{at } x = 0, \quad (6)$$

$$k_w \frac{\partial T_w}{\partial x}(x,t) = \frac{T_s(x,t) - T_w(x,t)}{r} \quad \text{at } x = 0, \quad (7)$$

where T_i, α_i, k_i, ρ_i and C_{pi} are the temperature, thermal diffusivity, thermal conductivity, density and specific heat of wall (for $i = w$) or solidified-material (for $i = s$), respectively. T_0 is the left-hand side wall surface temperature assumed constant, x is the space coordinate, h is the location of solid–liquid interface, t is time and L is the latent heat of solidification.

In the above system, equations (1) and (4) are the transient heat-conduction energy equations of wall and solidified-material, respectively. Equations (2) and (5) are boundary conditions, equation (3) is the energy balance at the solid–liquid interface, equations (6) and (7) are the energy balance equations at the wall–solid contact.

To prepare the foregoing model for a perturbation analysis, we recognize that the Stefan number, which signifies the importance of sensible heat to the latent heat, is less than unity and small compared to other variables in some phase-change problems, and therefore it can serve as a small perturbation parameter. After defining the dimensionless variables of temperature θ_i ($i = w$, for wall; $i = s$, for solid), space coordinate X, time τ, solid–liquid interface position H, speed of solid–liquid interface g, Stefan number ε, thermal resistance R, thermal conductivity β and thermal diffusivity ζ, as:

$$\theta_i = \frac{T_i - T_0}{T_f - T_0} \quad i = s \text{ or } w$$

$$X = \frac{x}{l}, \quad \tau = \frac{\varepsilon \alpha_s t}{l^2}, \quad H = \frac{h}{l}, \quad g = \frac{dH}{d\tau}$$

$$\varepsilon = \frac{C_{ps}(T_f - T_0)}{L}, \quad R = \frac{k_s r}{l}, \quad \beta = \frac{\alpha_s}{\alpha_w}, \quad \zeta = \frac{k_s}{k_w} \quad (8)$$

equations (1)–(7) will become:

$$\frac{\partial^2 \theta_s}{\partial X^2} = \varepsilon g \frac{\partial \theta_s}{\partial H}, \quad (9)$$

$$[\theta_s]_{X=H} = 1, \quad (10)$$

$$g = \left[\frac{\partial \theta_s}{\partial X}\right]_{X=H}, \quad (11)$$

$$\frac{\partial^2 \theta_w}{\partial X^2} = \varepsilon \beta g \frac{\partial \theta_w}{\partial H}, \quad (12)$$

$$[\theta_w]_{X=-1} = 0, \quad (13)$$

$$\left[\frac{\partial \theta_s}{\partial X}\right]_{X=0} = \left[\frac{\theta_s - \theta_w}{R}\right]_{X=0}, \quad (14)$$

$$\left[\frac{\partial \theta_w}{\partial X}\right]_{X=0} = \left[\zeta \frac{\theta_s - \theta_w}{R}\right]_{X=0}. \quad (15)$$

Assuming the magnitude of R, ζ and β are of order one, then perturbation solutions to the system can be written in general as

$$\theta_s = \theta_{s0} + \varepsilon\theta_{s1} + \varepsilon^2\theta_{s2} + \ldots, \quad (16)$$

$$\theta_w = \theta_{w0} + \varepsilon\theta_{w1} + \varepsilon^2\theta_{w2} + \ldots, \quad (17)$$

and

$$g = g_0 + \varepsilon g_1 + \varepsilon^2 g_2 + \ldots. \quad (18)$$

Substituting equations (16)–(18) into equations (9)–(15), we treat them order by order and get the following systems:

ε^0:

$$\frac{\partial^2 \theta_{s0}}{\partial X^2} = 0, \quad (19)$$

$$[\theta_{s0}]_{X=H} = 1, \quad (20)$$

$$g_0 = \left[\frac{\partial \theta_{s0}}{\partial X}\right]_{X=H}, \quad (21)$$

$$\frac{\partial^2 \theta_{w0}}{\partial X^2} = 0, \quad (22)$$

$$[\theta_{w0}]_{X=-1} = 0, \quad (23)$$

$$\left[\frac{\partial \theta_{s0}}{\partial X}\right]_{X=0} = \left[\frac{\theta_{s0} - \theta_{w0}}{R}\right]_{X=0}, \quad (24)$$

$$\left[\frac{\partial \theta_{w0}}{\partial X}\right]_{X=0} = \left[\zeta \frac{\theta_{s0} - \theta_{w0}}{R}\right]_{X=0}; \quad (25)$$

ε^1:

$$\frac{\partial^2 \theta_{s1}}{\partial X^2} = g_0 \frac{\partial \theta_{s0}}{\partial H}, \quad (26)$$

$$[\theta_{s1}]_{X=H} = 0, \quad (27)$$

$$g_1 = \left[\frac{\partial \theta_{s1}}{\partial X}\right]_{X=H}, \quad (28)$$

$$\frac{\partial^2 \theta_{w1}}{\partial X^2} = \beta g_0 \frac{\partial \theta_{w0}}{\partial H}, \quad (29)$$

$$[\theta_{w1}]_{X=-1} = 0, \quad (30)$$

$$\left[\frac{\partial \theta_{s1}}{\partial X}\right]_{X=0} = \left[\frac{\theta_{s1} - \theta_{w1}}{R}\right]_{X=0}, \quad (31)$$

$$\left[\frac{\partial \theta_{w1}}{\partial X}\right]_{X=0} = \left[\zeta \frac{\theta_{s1} - \theta_{w1}}{R}\right]_{X=0}; \quad (32)$$

ε^2:

$$\frac{\partial^2 \theta_{s2}}{\partial X^2} = g_0 \frac{\partial \theta_{s1}}{\partial H} + g_1 \frac{\partial \theta_{s0}}{\partial H}, \quad (33)$$

$$[\theta_{s2}]_{X=H} = 0, \quad (34)$$

$$g_2 = \left[\frac{\partial \theta_{s2}}{\partial X}\right]_{X=H}, \quad (35)$$

$$\frac{\partial^2\theta_{w2}}{\partial X^2}=\beta\left(g_0\frac{\partial\theta_{w1}}{\partial H}+g_1\frac{\partial\theta_{w0}}{\partial H}\right), \tag{36}$$

$$[\theta_{w2}]_{X=-1}=0, \tag{37}$$

$$\left[\frac{\partial\theta_{s2}}{\partial X}\right]_{X=0}=\left[\frac{\theta_{s2}-\theta_{w2}}{R}\right]_{X=0}, \tag{38}$$

$$\left[\frac{\partial\theta_{w2}}{\partial X}\right]_{X=0}=\left[\zeta\frac{\theta_{s2}-\theta_{w2}}{R}\right]_{X=0}. \tag{39}$$

If higher-order terms in the series are induced, the solutions will be more accurate. However, when the perturbation quantity is sufficiently small, higher-order terms can be neglected.

The solutions to the equations (19)–(39) are found to be:

$$\theta_{s0}=\frac{X+\eta}{H+\eta}, \tag{40}$$

$$\theta_{s1}=-\frac{1}{(H+\eta)^3}\left(\frac{1}{6}X^3+\frac{\eta}{2}X^2+C_1X+\eta C_1-\frac{\beta\zeta}{3}\right), \tag{41}$$

$$\theta_{s2}=D[A_0X^5+A_1X^4+A_2X^3+A_3X^2+C_2X+\eta C_2+\beta\zeta(B_0-B_1+B_2-B_3)], \tag{42}$$

$$\theta_{w0}=\frac{\zeta(X+1)}{H+\eta}, \tag{43}$$

$$\theta_{w1}=-\frac{\beta\zeta}{(H+\eta)^3}\left(\frac{1}{6}X^3+\frac{1}{2}X^2+\frac{C_1}{\beta}X+\frac{C_1}{\beta}-\frac{1}{3}\right), \tag{44}$$

$$\theta_{w2}=D\beta\zeta\left(B_0X^5+B_1X^4+B_2X^3+B_3X^2+\frac{C_2}{\beta}X+\frac{C_2}{\beta}+B_0-B_1+B_2-B_3\right), \tag{45}$$

and

$$g_0=\frac{1}{H+\eta}, \tag{46}$$

$$g_1=-\frac{1}{(H+\eta)^3}(\tfrac{1}{2}X^2+\eta X^2+C_1), \tag{47}$$

$$g_2=D(\tfrac{1}{5}A_0X^4+\tfrac{1}{4}A_1X^3+\tfrac{1}{3}A_2X^2+\tfrac{1}{2}A_3X+C_2), \tag{48}$$

where

$$\eta=R+\zeta, \tag{49}$$

$$C_1=\frac{2\beta\zeta-3\eta H^2-H^3}{6(H+\eta)}, \tag{50}$$

$$C_2=\frac{-[A_0H^5+A_1H^4+A_2H^3+A_3H^2+\beta\zeta(B_0-B_1+B_2+B_3)]}{H+\eta}, \tag{51}$$

$$A=H^3+3\eta H^2+3\eta^2H+\beta\zeta, \tag{52}$$

$$A_0=\tfrac{3}{20}(H+\eta), \tag{53}$$

$$A_1=\tfrac{3}{4}\eta(H+\eta), \tag{54}$$

$$A_2=\tfrac{1}{6}[3(H+\eta)(\eta^2+4C_1)+A], \tag{55}$$

$$A_3=\tfrac{1}{2}[3(H+\eta)(4\eta C_1-\beta\zeta)+A\eta], \tag{56}$$

$$B_0=\tfrac{3}{40}(H+\eta)(\beta+1), \tag{57}$$

$$B_1=\tfrac{1}{8}(H+\eta)(3\beta+2\eta+1), \tag{58}$$

$$B_2=\tfrac{1}{6}[3(H+\eta)(4C_1+\eta)+A], \tag{59}$$

$$B_3=\tfrac{1}{2}[3(4C_1-\beta)(H+\eta)+A], \tag{60}$$

$$D=\frac{1}{3(H+\eta)^6}. \tag{61}$$

The above analysis shows that the complex phase-change problem involving wall conduction and wall–material interfacial thermal resistance can be solved by using the perturbation method. The temperature distributions of wall and solidified-material as well as solidified speed can be expressed in analytical forms. The location of solid–liquid H can be calculated by Runge–Kutta method from equation (18). Evaluation of these quantities are straightforward and much simpler.

RESULTS AND DISCUSSION

The result of the case without the effects of wall conduction and wall–material interfacial thermal resistance can be seen in earlier works [5, 9, 11, 12]. The exact solutions are expressed as:

$$\theta_s=\frac{erf(\lambda X/H)}{erf(\lambda)}, \tag{62}$$

and

$$H=2\lambda\sqrt{\tau^*}, \tag{63}$$

where λ is a root of the equation:

$$\sqrt{\pi}\lambda e^{\lambda^2}erf(\lambda)=\varepsilon. \tag{64}$$

In the case of infinite heat transfer across the wall–material interface (neglecting the wall–material interfacial resistance), equations (6) and (7) of the energy balance equations at wall–solid contact will be changed into:

$$\zeta\left[\frac{\partial\theta_s}{\partial X}\right]_{X=0}=\left[\frac{\partial\theta_w}{\partial X}\right]_{X=0}, \tag{65}$$

$$[\theta_s]_{X=0}=[\theta_w]_{X=0}. \tag{66}$$

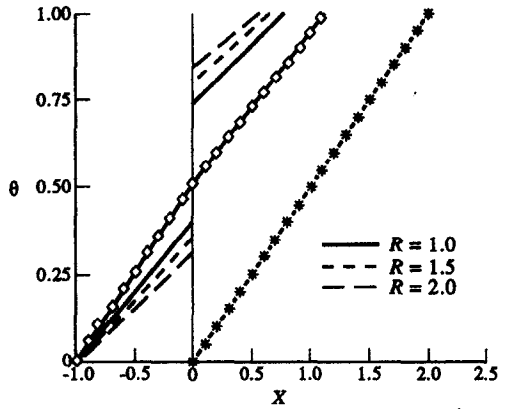

FIG. 2. Temperature distributions in the system for three values of R with $\varepsilon = 0.02$, $\zeta = 1.2$, $\beta = 1.2$ and $\tau^* = 100.0$ ($*-*$: the case ignoring the effects of wall conduction and wall–material interfacial thermal resistance, $\diamond-\diamond$: the case concerning wall conduction but ignoring the wall–material interfacial thermal resistance).

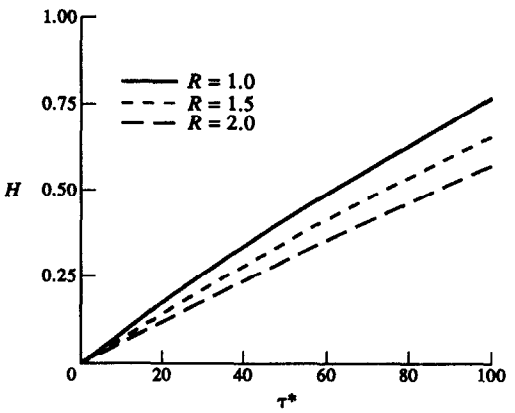

FIG. 3. Solid–liquid interface position vs time for three values of R with $\varepsilon = 0.02$, $\zeta = 1.2$ and $\beta = 1.2$.

The solutions can be derived by following the similar perturbation procedures and found to be the same as equations (40)–(61) but replacing η with ζ.

Figure 2 shows the temperature distributions of wall and solidified-material with different value of dimensionless wall–material interfacial resistance R for $\varepsilon = 0.02$, $\beta = 1.2$, $\zeta = 1.2$, and $\tau^* = 100.0$. It is easy to see that the speed of the solid–liquid interface is the highest in the case ignoring the effects of wall conduction and wall–material interfacial thermal resistance, while the case concerning wall conduction but ignoring the wall–material interfacial thermal resistance is second, and the case concerning both effects is the lowest. Furthermore, the temperature at any position of the solidified-material, θ_s, increases with increasing R, while the temperature at any position of the wall, θ_w, decreases with increasing R. In Fig. 3 the effect of varying wall–material interfacial resistance on solid–liquid interface position during the process is demonstrated for $\varepsilon = 0.02$, $\beta = 1.2$ and $\zeta = 1.2$. The solidification rate increases with decreasing R. The above behaviors can be explained from

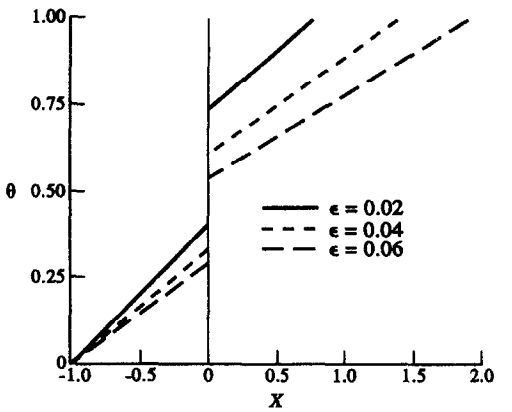

FIG. 4. Temperature distributions in the system for three values of ε with $R = 1.0$, $\zeta = 1.2$, $\beta = 1.2$ and $\tau^* = 100.0$.

the definition of the wall–material interfacial thermal resistance. As R is increased, the rate of energy transport across the wall–material interface decreases, and this leads to an increase in the net rate of heat gain from the boundary of the small local solidified-materials region and a decrease in that of the wall region. Consequently, its temperature responses are increased for solidified-material and decreased for wall. Consider equation (11) as the energy balance equation for the solid–liquid interface, in which the term of g expresses the speed of solid–liquid interface and the term of $\partial\theta_s/\partial X$ represents energy transport from the solid–liquid interface into solidified-material. As mentioned above, increasing R increases θ_s and so the rate of energy transport from solid–liquid interface to solid is decreased, which results in a decrease in the speed of the solid–liquid interface.

In Figs. 4 and 5 the effect of varying the Stefan number, ε, on the temperature and solid–liquid interface position are demonstrated, respectively. As ε is increased, the ratio of heat which can be stored within the solid to the heat released by solidification increases, and this leads to an increase in the solidified rate as well as a decrease in the net rate of heat gain from the boundary of the solid and an increase in that

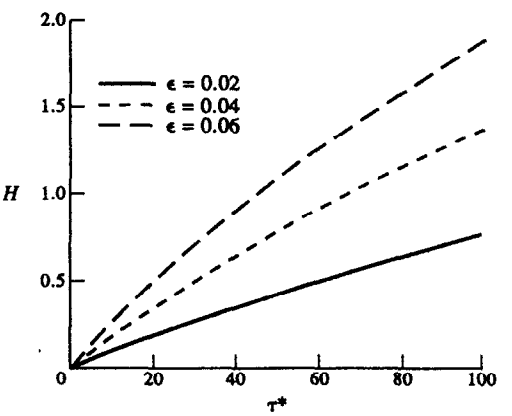

FIG. 5. Solid–liquid interface position vs time for three values of ε with $R = 1.0$, $\zeta = 1.2$ and $\beta = 1.2$.

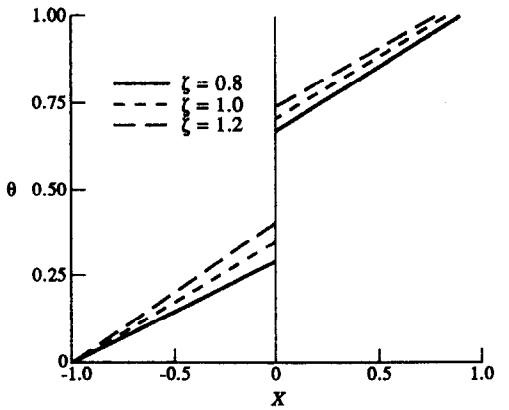

FIG. 6. Temperature distributions in the system for three values of ζ with $R = 1.0$, $\varepsilon = 0.02$, $\beta = 1.2$, and $\tau^* = 100.0$.

of the wall in order to maintain a constant R. So, increasing ε results in a decrease in θ_s and an increase in both θ_w and the speed of the solid–liquid interface.

Figures 6 and 7 show the effect of varying ζ, the ratio of solidified-material thermal conductivity to wall thermal conductivity, on the temperature and solid–liquid interface position. As ζ is decreased, the rate of energy transport across the wall increases, and this leads to an increase in the solidified rate and a decrease in the net rate of energy gain from the boundary of the wall region as well as the net rate of heat gain from the boundary of the solidified-material region. Consequently, decreasing ζ results in an increase in g and a decrease in both θ_s and θ_w.

To be appropriate for perturbation analysis, the selection of a perturbation parameter which is small compared to others is of importance. In most problems the perturbation quantity appears naturally in the equation and its choice is based on the physical understanding of the problem. The choice will then determine the simplicity or usefulness of the final solution. In phase-change literature, the Stefan number is usually selected as perturbation quantity. The magnitude of the Stefan number can vary considerably, depending on the material and the temperature difference involved. For water, it is less than unity; for metals it is of the order of 1–10 [13]. Thus, for substances such as water and for materials whose Stefan number is very small compared to other variables during the phase-change process, a perturbation method can be appropriately used. But, for metals such as the solidification of ingots, this perturbation analysis based on the assumption of a small Stefan number is not appropriate.

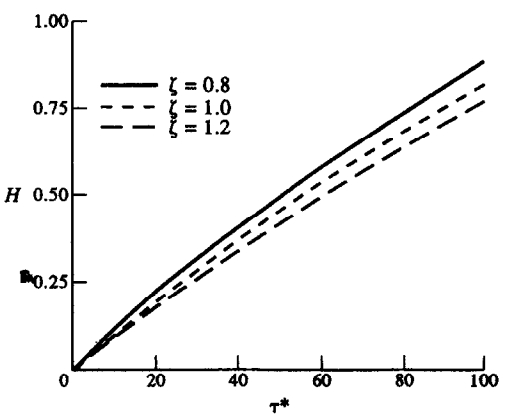

FIG. 7. Solid–liquid interface position vs time for three values of ζ with $R = 1.0$, $\varepsilon = 0.02$ and $\beta = 1.2$.

In the above procedures, the magnitude of R, ζ and β are assumed to be of order one for the appropriate perturbation analysis concerning equations (8)–(14). However, those quantities can vary arbitrarily because those variables can be written with another proper form within the mathematical equations. It is appropriate for the perturbation method.

CONCLUSIONS

In this work, it is seen that the perturbation technique presented here is simple to use to predict quantitative thermal information during the solidification process. Conclusions are summarized as:

(1) In the case without the effects of wall conduction and wall–material interfacial thermal resistance the solidification rate is the highest, while the case concerning wall conduction but ignoring the wall–material interfacical thermal resistance is second, and the case concerning both effects is the lowest.
(2) The temperature distributions of solidified-material during solidification will increase with increasing R, wall–material interfacial thermal resistance, or decreasing ε, Stefan number, or increasing ζ, the ratio of solidified-material thermal conductivity to wall thermal conductivity.
(3) The temperature distributions of the wall during solidification will increase with decreasing R, or increasing ε, or increasing ζ.
(4) The solidification rate will increase with decreasing R, or increasing ε, or decreasing ζ.

REFERENCES

1. A. Garcia and M. Prates, Mathematical model for the unidirectional solidification of metals: 1. Cooled molds, *Metallurgical Transactions B* **9**, 449–457 (1978).
2. A. Garcia, T. W. Clyne and M. Prates, Mathematical model for the unidirectional solidification of metals: 2. Massive molds, *Metallurgical Transactions B* **10**, 85–92 (1979).
3. T. W. Clyne and A. Garcia, Assessment of a new model for heat flow during unidirectional solidification of metals, *Int. J. Heat Mass Transfer* **23**, 773–782 (1980).
4. R. Viskanta, Heat transfer during melting and solidification of melts, *J. Heat Transfer* **110**, 1205–1219 (1988).
5. H. S. Carslaw and J. C. Jaeger, *Conduction of Heat in Solids* (2nd edition). Clarendon Press, Oxford (1959).
6. N. M. Ozisik, *Heat Conduction* (1st edition), Chapter 10. Wiley, New York (1980).
7. R. I. Pedroso and G. A. Domoto, Perturbation solution for spherical solidification of saturated liquids, *J. Heat Transfer* **95**, 42–46 (1973).

8. R. I. Pedroso and G. A. Domoto, Exact solution by perturbation method for planar solidification of a saturated liquid with convection at the wall, *Int. J. Heat Mass Transfer* **16,** 1816–1819 (1973).
9. C. L. Huang and Y. P. Shih, Perturbation solutions of planar diffusion-controlled moving-boundary problems, *Int. J. Heat Mass Transfer* **18,** 689–695 (1975).
10. M. M. Yan and P. N. S. Huang, Perturbation solutions to phase change problem subject to convection and radiation, *J. Heat Transfer* **101,** 96–100 (1979).
11. A. Aziz and T. Y. Na, *Perturbation Methods in Heat Transfer* (1st edition). Hemisphere, New York (1984).
12. A. Aziz and V. J. Lunardini, Perturbation techniques in phase change heat transfer, *ASME Appl. Mech. Rev.* **46,** 29–67 (1993).
13. A. D. Solomon, Mathematical modeling of phase change processes for latent heat thermal energy storage, Report No. ORNL/CSD-39, Union Carbide Corporation (1979).